Lock-in Detection and Hall Effect

Kyungmin Yu*
Department of Materials Science and Engineering,
Seoul National University
1, Gwanak-ro, Gwanak-gu, Seoul, Republic of Korea
E-mail: yukm0227@snu.ac.kr
(Dated: May 23, 2024)

Lock-in detection is a powerful method that extracts an original signal from the signal with noises. To conduct the lock-in detection, it is enough to pass the input signal through Double Balanced Mixer (DBM) and Low-Pass Filter (LPF), successively. In this experiment, the components that are used in the lock-in detection were studied and calibrated. During the calibration process, some anomalies in the components were found and the causes were analyzed. Then, the lock-in detection was conducted for the signal with noise, which is generated by a function generator and a noise generator. The results of the lock-in detection when the parameters in each circuit component change were analyzed. Finally, the magnetic field of a magnet was measured by performing the lock-in detection for the signal from a Hall sensor. The magnetic field generated by a magnet was at most 6 mT, and the magnetic dipole moment of the magnet was about $1\,\mathrm{J\,T^{-1}}$.

I. INTRODUCTION

Lock-in detection is a widely used method that can extract a signal with a certain frequency from a signal with noises. [1] Due to its simple procedure and great performance, lock-in detection can be applied in various fields. For instance, to analyze the Hall effect properly, eliminating noises from the detected signal is required since the magnitude of the signal and noises are comparable. To get rid of the noises, lock-in detection can be applied. In this experiment, some calibrations and analysis with a lock-in detector were conducted. After that, the Hall effect of a magnet was measured and analyzed by the properly calibrated lock-in detector.

A. Background: Lock-in Detection

Assume a sinusoidal signal containing sinusoidal noises with various angular frequencies. If two sinusoidal signals with angular frequencies ω_1 and ω_2 and amplitude A_1 and A_2 are multiplied, the output signal will be as follows.

$$\begin{aligned} &A_1 \sin(\omega_1 t) A_2 \sin(\omega_2 t) \\ &\quad = \frac{1}{2} A_1 A_2 (\cos(\omega_1 - \omega_2)t - \cos(\omega_1 + \omega_2)t) \end{aligned} \tag{1}$$

If ω_1 is not equal to ω_2, the time average of (1) is zero. The only case that the time average of (1) is nonzero is when $\omega_1 = \omega_2$. An ideal Low-Pass Filter (LPF) outputs a Direct Current (DC) signal of which amplitude is the time average of the input signal. When the signal (1) passes an ideal LPF, the output signal is always zero except the case of $\omega_1 = \omega_2$. Therefore, to extract a signal with a certain angular frequency ω, it is enough to multiply a sinusoidal signal with an angular frequency ω, and then pass the multiplied signal to the LPF. This process is called lock-in detection. Note that lock-in detection does not function well when the frequency of noise and the targeted frequency are similar, since the noise and the targeted signal are both included in the output signal. Therefore, lock-in detection can be used when the noise and the original signal have widely different frequencies. [1]

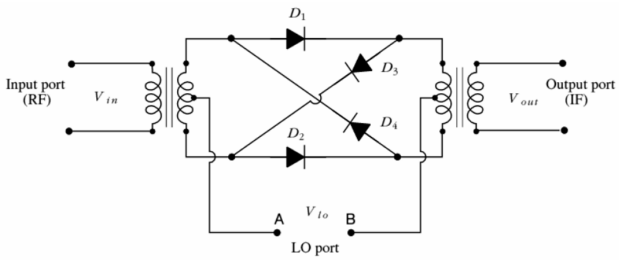

FIG. 1. The circuit diagram of double balanced mixer.

The function of the lock-in detector remains identical when the multiplied signal changes from a sine function to a sign function. In reality, the lock-in detection is usually performed by Double Balanced Mixer (DBM). In a DBM, the frequency of the reference signal can be set. When an input signal is given, DBM outputs the signal which is a product of the input signal and the sign function with the set frequency. In FIG. 1, the circuit diagram of DBM is depicted.

When the output signal of a DBM passes through the LPF, the DC signal only remains. The value of DC signal depends on the amplitude of the original signal with a certain frequency, as shown in (1). Based on the amplitudes of each frequency, the original signal can be reconstructed based on the Fourier transformation.

* Also at Department of Physics and Astronomy, Seoul National University. (Double major)

B. Background: Hall effect

When a conductor is subjected to the perpendicular electric current and magnetic field, the voltage difference is generated in the direction that is simultaneously perpendicular to the current and magnetic field. This phenomenon is termed the Hall effect, and the generated voltage difference is termed Hall voltage. [2] The charge carrier in the material is subjected to electric force by the Hall voltage and magnetic force. In the equilibrium, the magnitudes of two forces are the same. Let the Hall voltage be V_H, the drift speed of the carrier be v_d, the magnitude of the applied magnetic field be B, and the width of the specimen be d. Then, the equilibrium condition is as follows.

$$\frac{eV_H}{d} = eBv_d \tag{2}$$

Based on the microscopic description of the electric current, the electric current I can be written as (3), where S is a cross-section of the specimen, and n is a density of the charge carrier. [3]

$$I = Sev_d n \tag{3}$$

Combining (2) and (3), the magnitude of the Hall voltage is as follows.

$$V_H = \frac{id}{neA}B = R_H\frac{id}{A}B \tag{4}$$

R_H is termed Hall coefficient, which is defined by $1/ne$. From (4), the magnitude of the magnetic field B can be calculated. In this way, the Hall effect can be applied to measure the magnetic field from Hall voltage. Hall sensor enables the measurement of a magnetic field with the Hall effect. However, the magnitude of Hall voltage is so small that it is easily affected by noise. Lock-in detection is a great breakthrough to eliminate the noise and enables accurate magnetic field measurement.

II. MATERIALS AND METHODS

A. Calibration of Lock-in Detector Components

A function generator (GD-0020N, Protek Instument, Inc.) was employed to generate the input signal. Also, an oscilloscope (DPO2024, Tektronix, Inc.) was used to analyze signals. For the lock-in detection, Single Processor/Lock-in Amplifier (Teachspin, Inc.) was employed. The components in the detector must be properly calibrated before the experiment. The calibrated components are 1) pre-amplifier, 2) phase shifter, 3) DBM, and 4) LPF.

1. Pre-amplifier Calibration

A pre-amplifier receives an input signal and outputs the amplified signal. The amplitude ratio of output and input signals is termed gain, which can be set from 1 to 1000 in the apparatus. Since the high gain is not required and excessive amplification may cause a breakdown, the gain is set between 1 and 20 in this experiment. When the input signal frequency is not too high, the pre-amplifier functions well with a stationary gain. However, when the frequency exceeds a certain value, the gain starts decreasing linearly. To confirm this phenomenon and to set the input frequency for the lock-in detection, the gain values with different input frequencies were measured. The threshold frequency that is safe from the gain decrease was obtained with a linear regression.

2. Phase Shifter Calibration

A phase shifter receives an input signal and outputs the shifted signal with a certain phase difference. However, though the set phase difference is fixed, the actual phase shift changes as the input frequency differs. Especially, the phase shift changes linearly until a certain frequency, then it shows anomalies when the frequency exceeds the threshold. Therefore, the phase shifter must be calibrated before using it. Let the difference between the set phase shift in the apparatus and the actual phase shift be Δ. The Δ-frequency graph was plotted and the linear regression was conducted. For the high-frequency region where the linearity shows anomaly, the shape of the Δ-frequency curve was analyzed.

3. Checking DBM function

In the lock-in detector in this experiment, the DBM requires an input signal and a reference signal. If two signals have the same waveform with a certain phase difference, the DBM shows different output signals. For the phase difference $0, \pi/2, \pi$, and $3\pi/2$, the input and output of the DBM were compared.

4. LPF Calibration

In the LPF in the apparatus, its performance can be tuned by changing a roll-off and a time constant. When the signal passes through the LPF, the amplitude of the signal changes depending on the frequency. To analyze the tendency, the gain-frequency graph was plotted for possible roll-off values (6 dB/oct and 12 dB/oct) and time constant values (0.03 s, 0.1 s, and 0.3 s).

B. Lock-in Detection Measurement

For the lock-in detection, the original signal was generated by a function generator, and the noise was added by the noise generator in the apparatus. Since the form

of the generated noise is unknown, its naive form was analyzed by oscilloscope. In the oscilloscope, the automatic Fast Fourier Transform (FFT) function was employed to analyze the frequency-wise amplitude of the generated noise. Then, the original signal frequency was selected. Since the lock-in detection fails when the frequency of the noise and the original signal are similar, the frequency whose noise amplitude is small enough was selected.

After selecting the input frequency, the lock-in detection was performed. Based on the calibration result, the parameters such as the gain of the LPF and the pre-amplifier, the time constant of the LPF, and the roll-off of LPF were set. First, the output of LPF was plotted as a function of the set phase difference in the phase shifter. The plot was obtained with various amplitudes of the generated noise. Note that the phase difference with a maximum LPF output is the point that the two signals in DBM match well. The set phase difference with a maximum LPF output was applied in the following sections.

Lock-in detection can function well for the input signal with a DC offset. To confirm this, the original signal was generated with a certain value of DC offset from the function generator, then the lock-in detection was conducted for the noise-added signal.

C. Measurement of Magnetic Field of a Magnet

To measure the magnetic field of a magnet with the Hall effect, the noise must be canceled by lock-in detection. A Hall sensor is an apparatus that enables the measurement of a magnetic field based on the Hall effect. The Hall sensor in this experiment has four terminals, two for the measurement of the Hall voltage and the other two for applying current in the sensor. The current generated from the function generator was loaded in the Hall sensor, and then the lock-in detection was conducted for the measured Hall voltage. To measure the magnetic field of a given magnet, this process was repeated for the various distances between the magnet and the sensor. If the magnet is approximated to a single magnetic dipole with a magnetic dipole moment m, the magnetic field by the magnet is like (5). [4]

$$\vec{B}(r,\theta) = \frac{\mu_0 m}{4\pi r^3}(2\cos\theta\hat{r} + \sin\theta\hat{\theta}) \tag{5}$$

In this experiment, the box-shaped magnet was used. Its dimension is $14.70\,\text{mm} \times 12.80\,\text{mm} \times 4.05\,\text{mm}$. To consider a geometric factor of the magnet, the distance dependence of the magnetic field was measured for each face. Namely, the Hall sensor was placed at the center of the selected face, then it was moved carefully to maintain the alignment. The detailed fitting equation will be described in the following section.

III. RESULT

A. Calibration of Lock-in Detector Components

1. Pre-amplifier Calibration

The actual voltage gain of the pre-amplifier versus the frequency of the input signal for the possible gains (1, 2, 5, 10, 20) was plotted in FIG. 2. The gain was maintained similar to the value shown in the apparatus for the low-frequency region. However, as the frequency increased, the gain increased a little, then it rapidly dropped when the frequency exceeded a certain value, as shown in FIG. 2.

The voltage gain can be transformed as a decibel unit, where the transformation formula is as follows. Note that the coefficient is 20 to compensate that the power is proportional to the square of the voltage.

$$g_{\text{dB}} = 20\log_{10}\frac{V_{\text{out}}}{V_{\text{in}}} \tag{6}$$

If the voltage gain with a decibel unit drops by 3 dB, it means the actual voltage gain becomes $1/\sqrt{2}$ compared to the original gain. Since the power is proportional to the square of the voltage, the power delivered by the signal becomes half of the anticipated value at the 3 dB frequency. The frequency whose actual gain drops by 3 dB compared to the set gain is termed 3 dB frequency. Therefore, the 3 dB frequency can be set as the upper bound of the frequency whose gain is maintained stationary. With the linear regression in the region where the voltage gain drops linearly, the equation of the trend line and the 3 dB voltage were calculated, and shown in FIG. 2.

As shown in FIG. 2, the 3 dB frequencies were higher than 500 kHz. To avoid the anomaly of gain in the pre-amplifier, it is enough to set the input signal frequency lower than 500 kHz.

2. Phase Shifter Calibration

The phase shift value was set to be 45° in the apparatus. Then, the actual phase shift was measured by the oscilloscope with various input signal frequencies. Δ (i.e. the difference between the actual phase shift and the set phase shift) versus the frequency was plotted in FIG. 3. Since the oscilloscope can show the phase difference in the range from $-\pi$ to π, an appropriate value in the form of $2n\pi$ (n be an integer) was added for each data. In FIG. 3, Δ shows a linear change as the frequency increases, then the linearity disappears when the frequency is about 10 kHz. For the frequency range that linearity exists, the linear regression was conducted and the trend line was shown as a red dotted line.

In FIG. 3, the anomaly occur over 10 kHz. The region where this anomaly occurs is termed a linear region. For

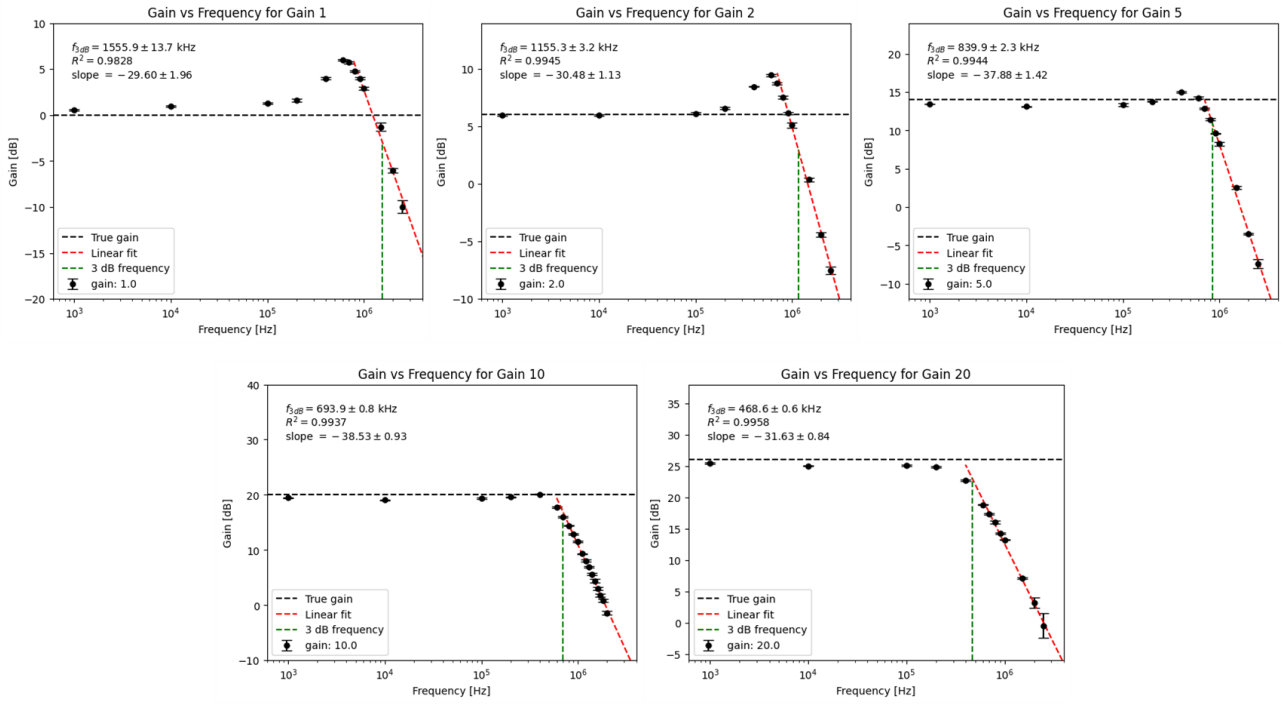

FIG. 2. The actual gain of the pre-amplifier versus the frequency of the input signal.

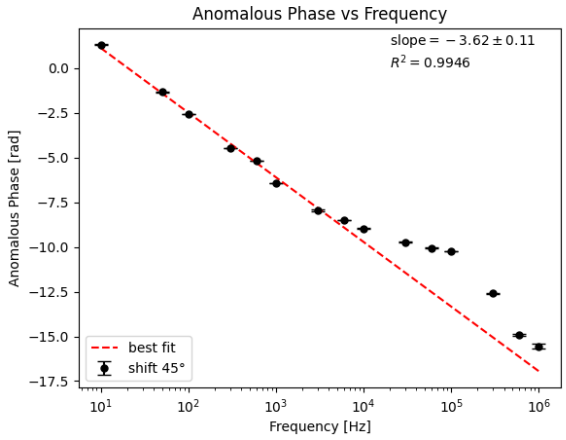

FIG. 3. Δ versus the frequency of the input signal.

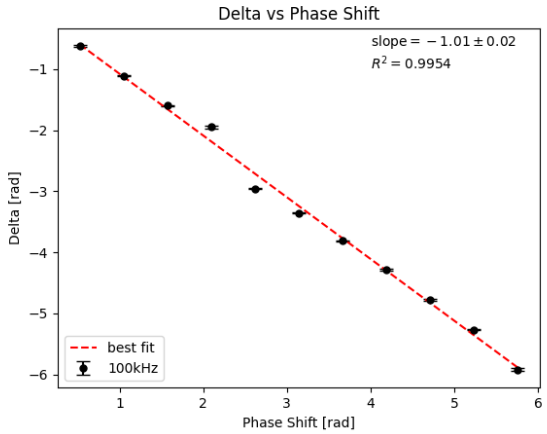

FIG. 4. Δ versus the set phase shift when the frequency of the input signal is 100 kHz.

instance, 100 kHz is in the linear region. When the frequency is 100 kHz, Δ versus the set phase shift in the apparatus was plotted in FIG. 4. The linear trend line was shown as a red dotted line.

In FIG. 4, the set phase shift and Δ change with almost identical rates, as shown in the slope of the trend line which is almost -1. Considering the definition of Δ, it implies that the actual phase shift is almost stationary though the set phase shift is changed in the apparatus. Namely, the phase shifter does not function well in the linear region. Also, the actual phase shift deviates much from the set phase shift. Therefore, referring to the oscilloscope data is required to set the proper phase shift.

3. Cheking DBM Function

To confirm that the DBM outputs the original signal multiplied by the sign function of the reference signal, two identical sinusoidal signals with a certain phase difference were given to the DBM. The signals shown in the oscilloscope display are shown in FIG. 5. The blue waveform is the original signal; the yellow waveform is

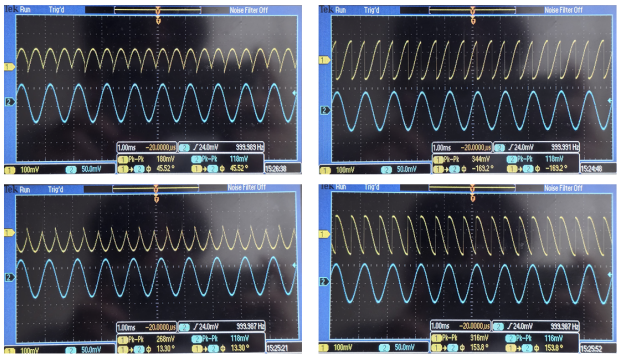

FIG. 5. The original signal (blue) and the output signal of the DBM (yellow) for the phase difference of 0 (top left), $\pi/2$ (top right), π (bottom left), and $3\pi/2$ (bottom right).

the output signal of the DBM.

Considering the function of the DBM, the sign function with a certain phase shift is multiplied by the original signal. If the phase shift is 0, the sign function changes the sign of the negative part of the original signal. The result is shown in the top left of FIG. 5, where the DBM outputs the signal in the form of $|\sin \omega t|$. In the same way, the sign function changes the sign of the positive part of the original signal when the phase difference is π. In this case, the DBM output is in the form of $-|\sin \omega t|$. If the phase difference is $\pi/2$ or $3\pi/2$, the increasing parts (or the decreasing parts) of the sinusoidal function change the sign by the sign function. The result is shown in the two right figures in FIG. 5. Therefore, it can be concluded that the DBM functions well as anticipated.

4. LPF Calibration

The time constant and roll-off dependence of the LPF frequency response is shown in FIG. 6. The frequency response of the LPF can be analyzed based on the circuit diagram. The right circuit diagram of FIG. 6 shows the simplest structure of an LPF. Theoretically, the voltage gain is described as follows. [5]

$$\begin{aligned} \frac{V_{\text{out}}}{V_{\text{in}}} &= \frac{X_C}{\sqrt{X_C^2 + R^2}} \\ &= \frac{1}{\sqrt{1 + (\omega RC)^2}} = \frac{1}{\sqrt{1 + (\omega\tau)^2}} \end{aligned} \tag{7}$$

From (7), the frequency dependence of the gain was obtained. If a time constant, which is defined by $\tau = RC$, is higher, the gain decreases more rapidly for the high-frequency input. This tendency can be easily checked in FIG. 6. To sum up, the effect of a time constant matches well with the experimental result.

Meanwhile, a roll-off determines the slope of gain decrease in the high-frequency region. In the high-frequency region where the approximation $\omega\tau \gg 1$ holds, the gain in (7) can be simplified into (8).

$$\frac{V_{\text{out}}}{V_{\text{in}}} \simeq \frac{1}{\omega\tau} \tag{8}$$

A roll-off is defined by the gain ratio for two different angular frequencies. Of course, it can be formulated with a dB unit. For two angular frequencies in octave, the roll-off can be described with a dB unit like (9).

$$\text{roll off [dB]} = 20 \log \frac{g_2}{g_1} = 20 \log 2 \simeq 6 \,[\text{dB/oct}] \tag{9}$$

For the simple LPF as shown in FIG. 6, the roll-off is approximately 6 regardless of resistance and capacitance. However, if more than two simple LPFs are combined in sequence, the roll-off can be multiplied by the number of concatenated LPFs. Namely, the roll-off is 12 when two LPFs are concatenated. [6]

In FIG. 6, the slope of the high-frequency region is larger for the 12 dB/oct case. However, the slope is not identical to the exact roll-off value. The deviation from the theoretical value is much larger in the 12 dB/oct case. This error seems to stem from the contact resistance when two LPFs are contacted in the 12 dB/oct case. When the contact resistance is included in the circuit, the voltage in each terminal changes, and then the final gain is affected by the contact resistance. The actual circuit structure must be investigated to analyze the detailed error source.

B. Lock-in Detection Measurement

Since the lock-in detection does not work well when the frequency of noise is similar to that of the original signal, the amplitude distribution of the noise generator needs to be observed. The amplitude distribution of the noise is shown in FIG. 7a and FIG. 7b with FFT function in the oscilloscope. Note that the peak-to-peak voltage of the input signal was 100 mV and its frequency was 1 kHz.

As shown in FIG. 7a and FIG. 7b, most of the generated noise has a low frequency given that the noise peak is shown in the low-frequency region. Also, the overall fluctuation due to the noise gets larger when the noise intensity increases. Based on the amplitude distribution, the frequency of the generated signal was selected as 2 kHz.

Next, the lock-in detector output with the phase shift change was measured. The phase shifter was applied to plot the lock-in detector output with a certain phase shift. This process is essential since the phase of the input signal changes when it passes through the pre-amplifier. This phase shift must be recovered through the phase shifter. However, as shown in FIG. 3, the phase shifter does not function as written in the apparatus. Therefore, the value of the phase shifter must be set empirically. To perform the lock-in detection well, the input

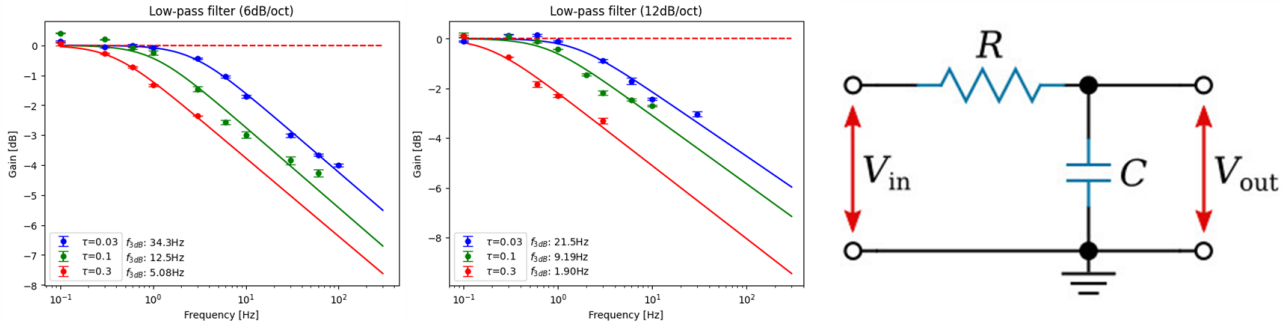

FIG. 6. The frequency response of the LPF for the roll-off of 6 dB/oct (left) and 12 dB/oct (middle). The circuit diagram of an LPF (right).

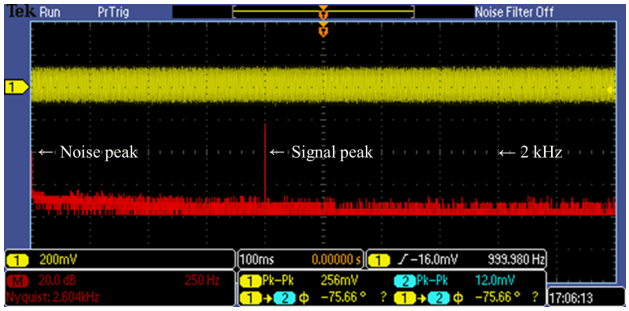

FIG. 7a. The amplitude distribution of the noise when the noise intensity is 10^{-4}.

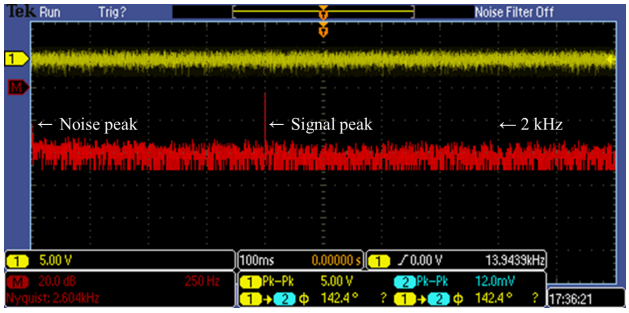

FIG. 7b. The amplitude distribution of the noise when the noise intensity is 10^{-2}.

signal and the reference signal must have an identical phase. When the phases match well, the lock-in detector output is maximized. Therefore, the phase difference that maximizes the lock-in detector output was applied for the following experiments. Note that the input signal frequency was 2 kHz, the peak-to-peak voltage was 1 V, the pre-amplifier gain was 2, the LPF gain was 2, and the LPF condition was 6 dB/oct, 12 s. The process was repeated for three kinds of noise intensities, 10^{-1}, 10^{-3}, and 10^{-5}. The result is shown in FIG. 8. In FIG. 8, the lock-in detector output was maximized when the phase shift was 225°. Since the frequency was maintained to be 2 kHz for the following experiments, this phase shift value was fixed, too.

In FIG. 8, the phase difference dependence of the lock-in detection output is sinusoidal. Let the input signal be sinusoidal with an angular frequency ω and an amplitude A. Assume that the reference signal has the same waveform as the input with a phase difference ϕ. If two signals pass through the DBM, the multiplication of two signals, $f(t)$ is like (10).

$$\begin{aligned} f(t) &= A\sin\omega t \times \mathrm{sgn}(\sin(\omega t+\phi)) \\ &= A\sin\omega t \times \mathrm{sgn}(\sin\omega t\cos\phi + \cos\omega t\sin\phi) \\ &= A[\cos\phi|\sin\omega t| + \sin\phi\sin\omega t\,\mathrm{sgn}(\cos\omega t)] \end{aligned} \tag{10}$$

If a signal like (10) passes through the LPF, the DC signal whose amplitude is the time average is obtained. The amplitude $V_m(\phi)$ of the output can be expressed like (11).

$$V_m(\phi) = \frac{A\cos\phi}{2\pi}\int_0^{2\pi/\omega} |\sin\omega t|dt = \frac{2A\cos\phi}{\pi} \tag{11}$$

Therefore, the lock-in detector output has a sinusoidal ϕ-dependence, as shown in (11).

In addition, the maximum value matches well with (11). The overall gain was 4 (2 from the pre-amplifier, 2 from the LPF) and the peak-to-peak voltage was 1 V. Therefore, the signal amplitude was 2 V, assuming the perfect sinusoidal wave. Therefore, the theoretical maximum of the lock-in output is about 1.273 V, which is $2/\pi$ times the signal amplitude. Referring to FIG. 8, this value matches well with the experimental data.

Finally, the noise with a DC offset was also under the lock-in detection. As shown in FIG. 9, the gain of the lock-in detection was maintained stationary regardless of the amplitude of the DC offset in the noise. Therefore, the DC stability of the lock-in detection was confirmed well.

C. Measurement of Magnetic Field of a Magnet

The magnetic field generated by a magnet is shown in FIG. 10. The fitting was conducted based on the theory of classical electrodynamics to obtain the magnetic dipole moment of the magnet. Assume that the

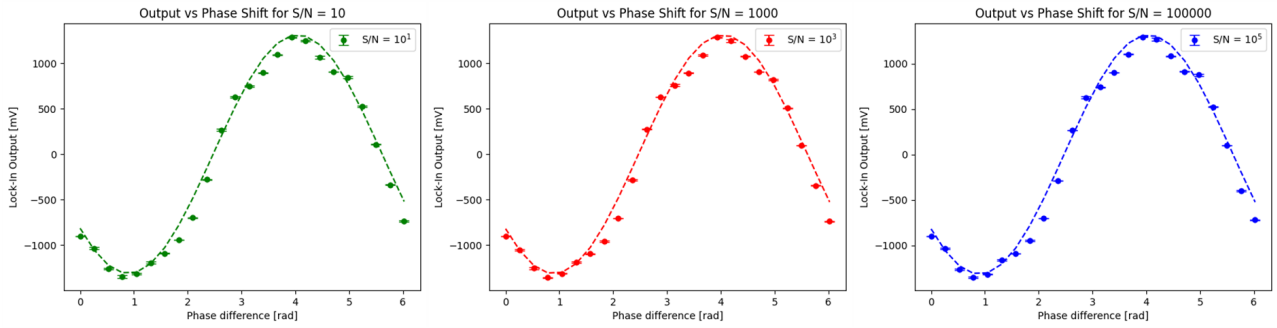

FIG. 8. The lock-in detector output with different phase shift values.

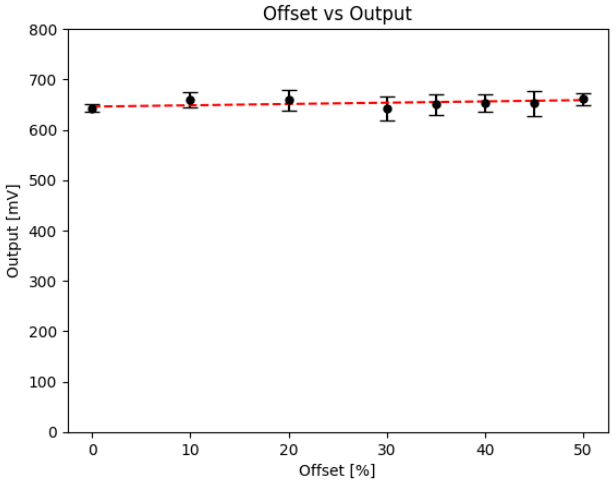

FIG. 9. The lock-in detector output when the noise includes the DC offset.

box-shaped magnet has a uniform magnetic dipole moment density within its volume, and the direction of the magnetic dipole moment is perpendicular to the widest face (face 1). Also, let the dimension of the magnet be $a \times b \times h (a > b > h)$, and the distance from one widest face of the magnet be z. Then, the magnetic field generated by this box-shaped magnetic dipole, $B(z)$, can be expressed like (12).

$$B(z) = \frac{\mu_0 m}{abh\pi}\left[\arctan\frac{ab}{2z\sqrt{4z^2+a^2+b^2}} - \arctan\frac{ab}{2(z+h)\sqrt{4(z+h)^2+a^2+b^2}}\right] \tag{12}$$

Based on (12), the fitting was conducted with parameters m, which is the magnetic dipole moment per unit volume. The fitting curve was shown in red dotted line in FIG. 10.

The obtained magnetic dipole moment value for each face is $1.27\,\mathrm{J\,T^{-1}}$, $1.59\,\mathrm{J\,T^{-1}}$, and $0.76\,\mathrm{J\,T^{-1}}$, respectively. This value matches well with the magnetic property of the neodymium magnet. The typical neodymium magnet has a magnetization (i.e. magnetic dipole moment per unit volume) from $600\,\mathrm{kA\,m^{-1}}$ to $2000\,\mathrm{kA\,m^{-1}}$. [7] Since the dimension of the magnet in this experiment is $14.70\,\mathrm{mm} \times 12.80\,\mathrm{mm} \times 4.05\,\mathrm{mm}$, the magnetic dipole moment of the whole magnet is between $0.457\,\mathrm{J\,T^{-1}}$ and $1.52\,\mathrm{J\,T^{-1}}$. The obtained magnetic dipole moment values are included in this range considering an error. However, the obtained magnetic dipole moment seems to be inaccurate. The overall fluctuations and errors are quite large, referring to the 1σ error bar in FIG. 10. The reason of this large error will be analyzed in the following section.

IV. DISCUSSION

A. Anomalies in the Circuit Components

1. *Pre-amplifier*

In the pre-amplifier, the gain was maintained well when the frequency was lower than a certain threshold; after the threshold, a slight increase followed by a rapid decline occurred. This phenomenon stems from the non-ideality of the amplifier. The practical circuit diagram of a common amplifier is shown in FIG. 11.

In FIG. 11, the capacitors function as a certain filter. Also, in the transistor, there is a built-in capacitor which also acts as a filter. Among these capacitors, C_{C1}, C_{C2}, and C_s function as a High-Pass Filter (HPF) since they lessen the output voltage when a signal frequency is low. On the contrary, the built-in capacitor in the transistor is known to function as an LPF. Therefore, in an amplifier, there is a certain frequency range such that the amplifier gives a stationary gain. This range is termed bandwidth, which is a difference of 3 dB frequency of a high-frequency regime and a low-frequency regime. [5] During the calibration of the amplifier, the high-frequency regime of the amplifier was under observation. Therefore, the gain decreased rapidly when the frequency was higher than a certain threshold.

In FIG. 2, it is also possible to observe that the 3 dB frequency for each gain decreases as the gain increases. It is a natural phenomenon since the built-in capacitor

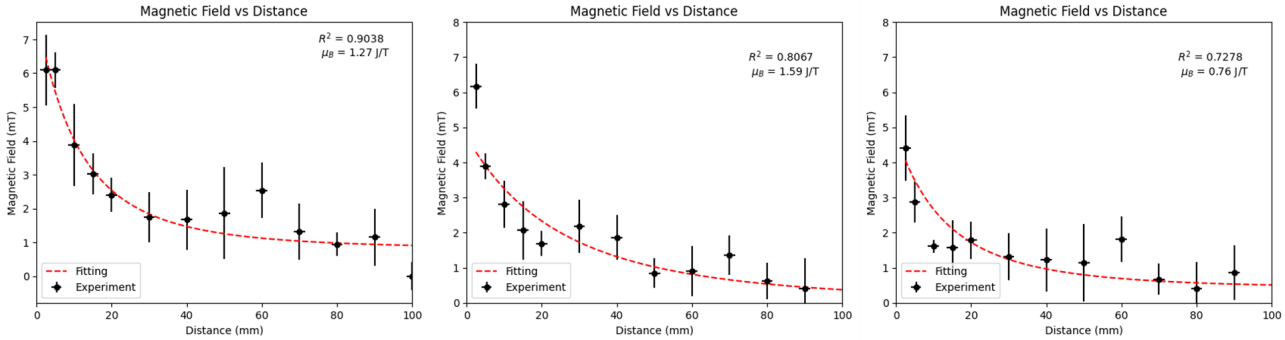

FIG. 10. The magnetic field generated by a magnet, for the face 1 (14.70 mm × 12.80 mm) (left), face 2 (14.70 mm × 4.05 mm) (middle), and face 3(12.80 mm × 4.05 mm).

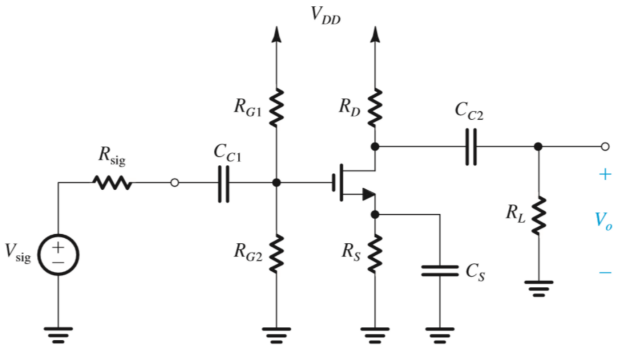

FIG. 11. The circuit diagram of a practical amplifier. [5]

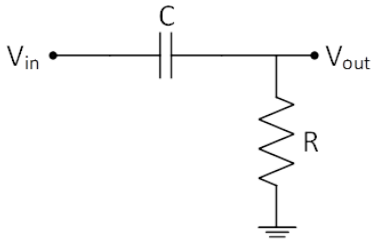

FIG. 12. The circuit diagram of a simple phase shifter.

in the transistor always has the same capacitance, unless the transistor is replaced. Therefore, the reactance of the built-in capacitor is identical. If the input voltage is identical, the voltage on the built-in capacitor is the same. (Note that the input voltage was maintained to be 100 mV for all the gains.) The gain is tuned by changing R_L in FIG. 11. To obtain a higher gain, R_L must be tuned smaller, and then the gain is affected more by the reactance of the built-in capacitor. Therefore, the 3 dB frequency is lower for the higher-gain case.

2. *Phase Shifter*

The phase shifter also showed some anomalies as shown in FIG. 3. The anomalies can be analyzed based on the circuit structure of the phase shifter. A basic principle of a phase shifter is a phase difference generated in an RLC circuit. For instance, the simplest phase shifter constructed by a resistor and a capacitor is shown in FIG. 12. To generate a phase shift greater than 180°, more than two phase shifters in FIG. 12 should be concatenated.

However, the phase shift generated by the simple phase shifter depends on the frequency. Namely, in an RLC series circuit, the phase difference between a current (which generates an output voltage) and an input voltage is as follows.

$$\phi = \arctan \frac{X_C}{R} = \arctan \frac{1}{\omega C R} \tag{13}$$

Therefore, the phase shift has a frequency dependence as shown in FIG. 3.

To tune the value of the phase shift, it is enough to tune the value of resistance in the phase shifter. However, when the frequency gets higher, the reactance of the capacitor decreases to 0, and then the phase difference does not change much when R is tuned. It is clear to put $\omega \to \infty$ in (13). Therefore, in the high-frequency regime, the actual phase shift is maintained stationary, as shown in FIG. 4.

B. Measurement of Magnetic Field of a Magnet

As mentioned in section III C, a large error occurred during the magnetic field measurement. Though the lock-in detection was performed to remove the noise, the intensity of the signal due to the Hall effect was still small. Therefore, a significant error is inevitable due to the small signal. In addition, there are some sources of external magnetic fields, such as conducting wires, electronic devices, and the earth's magnetic field. The measured signal may fluctuate when electronic devices or conducting wires move near the Hall sensor. The lock-in output fluctuated much during the measurement, so accurately reading the value was challenging. Also, the

earth's magnetic field, whose magnitude is from 25 mT to 65 mT, is comparable to the scale of the measured magnetic field. It means the earth's magnetic field has enough magnitude to affect the experimental result.

Furthermore, the microscopic structure of the magnet is unknown. In the fitting, the magnetic dipole moment in the magnet was assumed to be uniform, and pointing a certain direction. However, in reality, this can't be achieved due to defects inside the magnet. It is impossible to consider all the defects in the magnet, and the error due to the microstructure is inevitable. For the extended study to model the microscopic factor of the magnet, some methodologies in computational materials science such as Density Functional Theory (DFT) can be applied. Even if the magnetic dipole moment inside the magnet is assumed to be uniform, there is still an unresolved problem. In (12), the magnetic dipole moment was set to be perpendicular to the face whose dimension is $a \times b$. However, this assumption might be wrong since the actual magnetic dipole moment direction is unknown. The magnet applied in this experiment was box-shaped. Unlike a general bar magnet, the dipole moment direction (i.e. N pole and S pole) are not distinguished well for a flat magnet. For a more accurate fitting, the direction of the magnetic dipole moment can be considered. However, the overall data has a large fluctuation, and other errors are still large, so such fitting was not conducted.

To improve the magnetic field measurement, the apparatus that can align the components must be prepared. Due to the lack of an anchor during the measurement, the magnet was trembled slightly and not aligned well. This seems to be one of the error sources and must be improved with the preparation of a proper apparatus. Also, the inevitable error sources described above might be improved with some high-performance apparatus or advanced modelling.

V. CONCLUSION

The components of the lock-in amplifier were calibrated well, and their anomalies were analyzed. Many anomalies seem to stem from the capacitor in the circuit, which gives a certain frequency dependence. The lock-in detection was simulated with a phase generator and a noise generator. It was confirmed that the lock-in detection output has a sinusoidal phase dependence, which is consistent with the theory. Also, a DC offset of an input signal does not affect the lock-in detection much. Finally, the magnetic field generated by a magnet was carefully measured by the lock-in detection. The scale of the magnetic field generated by the magnet was at most 6 mT. It was tried to obtain the magnetic dipole moment of the magnet, however, the inevitable error sources and unknown microscopic structure of the magnet interrupted to obtain the accurate value. The rough scale of the magnetic dipole moment of the magnet was $1\,\mathrm{J\,T^{-1}}$.

ACKNOWLEDGMENTS

I appreciate performing this harsh experiment with my dear coworkers, Seunghyun Moon and Gyujin Kim.

[1] D. Blair and P. Sydenham, Phase sensitive detection as a means to recover signals buried in noise, Journal of Physics E: Scientific Instruments **8**, 621 (1975).
[2] C. Hurd, *The Hall effect in metals and alloys* (Springer Science & Business Media, 2012).
[3] D. Halliday, R. Resnick, and J. Walker, *Fundamentals of physics* (John Wiley & Sons, 2013).
[4] D. J. Griffiths, *Introduction to electrodynamics* (Cambridge University Press, 2023).
[5] J. W. Nilsson and S. A. Riedel, *Electric circuits* (Pearson Education Limited, 2020).
[6] J. M. Jacob, Advanced ac circuits and electronics: principles & applications, (No Title) (2004).
[7] D. R. Lide, *CRC handbook of chemistry and physics*, Vol. 85 (CRC press, 2004).